



**HAL**  
open science

## Bacterial capsular polysaccharides with antibiofilm activity share common biophysical and electrokinetic properties

Joaquín Bayard-Bernal, Jérôme Thiebaud, Marina Brossaud, Audrey Beaussart, Celine Caillet, Yves Waldvogel, Laetitia Travier, Sylvie Létoffé, Thierry Fontaine, Bachra Rokbi, et al.

► **To cite this version:**

Joaquín Bayard-Bernal, Jérôme Thiebaud, Marina Brossaud, Audrey Beaussart, Celine Caillet, et al.. Bacterial capsular polysaccharides with antibiofilm activity share common biophysical and electrokinetic properties. 2022. hal-03805110v1

**HAL Id: hal-03805110**

**<https://hal.univ-lorraine.fr/hal-03805110v1>**

Preprint submitted on 13 Oct 2022 (v1), last revised 31 May 2023 (v2)

**HAL** is a multi-disciplinary open access archive for the deposit and dissemination of scientific research documents, whether they are published or not. The documents may come from teaching and research institutions in France or abroad, or from public or private research centers.

L'archive ouverte pluridisciplinaire **HAL**, est destinée au dépôt et à la diffusion de documents scientifiques de niveau recherche, publiés ou non, émanant des établissements d'enseignement et de recherche français ou étrangers, des laboratoires publics ou privés.



Distributed under a Creative Commons Attribution - NonCommercial - NoDerivatives 4.0 International License

# Bacterial capsular polysaccharides with antibiofilm activity share common biophysical and electrokinetic properties

Joaquín Bayard-Bernal<sup>1,2</sup>, Jérôme Thiebaud<sup>3</sup>, Marina Brossaud<sup>3</sup>, Audrey Beaussart,<sup>4</sup> Celine Caillet,<sup>4</sup> Yves Waldvogel,<sup>4</sup> Laetitia Travier<sup>1,5</sup>, Sylvie Létouffé<sup>1</sup>, Thierry Fontaine<sup>6</sup>, Bachra Rokbi<sup>3</sup>, Philippe Talaga<sup>3</sup>, Christophe Beloin<sup>1</sup>, Noelle Mistretta<sup>3\*</sup>, Jérôme F.L. Duval<sup>4\*</sup> and Jean-Marc Ghigo<sup>1\*</sup>

<sup>1</sup> Institut Pasteur Université Paris Cité, CNRS UMR 6047, Genetics of Biofilms laboratory, Paris F-75015, France.

<sup>2</sup>Departamento de Genética, Facultad de Biología, Universidad de Sevilla, Apartado 1095, 41080 Sevilla, Spain.

<sup>3</sup>Sanofi, Research & Development, Campus Mérieux, 1541 avenue Marcel Mérieux, 69280, Marcy l'Etoile, France.

<sup>4</sup> Université de Lorraine, CNRS, Laboratoire Interdisciplinaire des Environnements Continentaux (LIEC), F-54000 Nancy, France.

<sup>5</sup> Institut Pasteur, Université Paris Cité, Inserm U1224, Brain-Immune Communication group, F-75015 Paris, France.

<sup>6</sup> Institut Pasteur, Université Paris Cité, INRAE, USC2019, Fungal Biology and Pathogenicity laboratory, F-75015 Paris, France.

**\*Co-corresponding authors:** Jérôme F.L. Duval; Noelle Mistretta, Jean-Marc Ghigo

**Email:** [Noelle.Mistretta@sanofi.com](mailto:Noelle.Mistretta@sanofi.com); [jerome.duval@univ-lorraine.fr](mailto:jerome.duval@univ-lorraine.fr); [jmghigo@pasteur.fr](mailto:jmghigo@pasteur.fr)

## **AUTHOR CONTRIBUTIONS:**

J. B.-B., N.M., P.T., J.F.L.D. and J.-M.G. designed the experiments. L.T., C.B. and B.R. contributed to the initial experiments. J. B.-B., J.T., M.B., A.B., C.C., Y.W., J.-M.G. and P.T. performed the experiments. J. B.-B., J.T., M.B., A.B., P.T., N.M., J.F.L.D. and J.-M.G. analyzed the data. J. B.-B., J.F.L.D. and J.-M.G. wrote the paper with significant contribution from C.B. J.T., A.B., P.T., B.R. and N.M.

**Competing Interest Statement:** The authors declare no competing financial interests. J.T. M. B. B. R., P. T. and N. M. are Sanofi employees and may hold shares and/or stock options in the company.

**Classification:** Biological Sciences, Microbiology; / Physical Sciences, Biophysics

**Keywords:** Biofilms; antibiofilm; biosurfactants; soft macromolecule electrokinetics

## **This PDF file includes:**

Main Text  
Figures 1 to 5  
Table 1

1 **Abstract**

2

3 Bacterial biofilms are surface-attached communities that are difficult to eradicate  
4 due to a high tolerance to antimicrobial agents. The use of non-biocidal surface-  
5 active compounds to prevent the initial adhesion and aggregation of bacterial  
6 pathogens is a promising alternative to antibiotic treatments and several  
7 antibiofilm compounds have been identified, including some capsular  
8 polysaccharides released by various bacteria. However, the lack of chemical and  
9 mechanistic understanding of the activity of these high-molecular-weight  
10 polymers limits their use for control of biofilm formation. Here, we screened a  
11 collection of 32 purified capsular polysaccharides and identified seven new  
12 compounds with non-biocidal activity against biofilms formed by *Escherichia coli*  
13 and/or *Staphylococcus aureus*. We analyzed the polysaccharide mobility under  
14 applied electric field conditions and showed that active and inactive  
15 polysaccharide polymers display distinct electrokinetic properties and that all  
16 active macromolecules shared high intrinsic viscosity features. Based on these  
17 characteristics, we identified two additional antibiofilm capsular polysaccharides  
18 with high density of electrostatic charges and their permeability to fluid flow. Our  
19 study therefore provides insights into key biophysical properties discriminating  
20 active from inactive polysaccharides. This characterization of a specific  
21 electrokinetic signature for polysaccharides displaying antibiofilm activity opens  
22 new perspectives to identify or engineer non-biocidal surface-active  
23 macromolecules to control biofilm formation in medical and industrial settings.

24

25

26

## 1 **Significance statement**

2 Some bacteria produce non-biocidal capsular polysaccharides that reduce the  
3 adhesion of bacterial pathogens to surfaces. Due to a lack of molecular and  
4 structural definition, the basis of their antiadhesion activity is unknown, thus  
5 hindering their prophylactic use for biofilm control. Here, we identified nine new  
6 active compounds and compared their composition, structure and biophysical  
7 properties with other inactive capsular polysaccharides. Despite the absence of  
8 specific molecular motif, we demonstrate that all active polysaccharides share  
9 common electrokinetic properties that distinguish them from inactive polymers.  
10 This characterization of the biophysical properties of antibiofilm bacterial  
11 polysaccharide provides key insights to engineer non-biocidal and bio-inspired  
12 surface-active compounds to control bacterial adhesion in medical and industrial  
13 settings.

14

15

1 **MAIN TEXT**

2

3 **Introduction**

4

5 Bacterial biofilms are widespread surface-attached or aggregated bacteria that  
6 can negatively impact human activities when developing on medical or industrial  
7 surfaces (1, 2). Due to their high tolerance to antibiotics, biofilms are difficult to  
8 eradicate and the prevention of biofilm-associated infections is a major health  
9 and economic issue (3, 4). Strategies to prevent biofilm formation often targets  
10 the initial steps of bacterial adhesion using surfaces coated by biocidal agents  
11 such as broad-spectrum antibiotics or heavy metals (5). These approaches are  
12 limited by the rapid masking of the coated surfaces by bacterial and organic  
13 debris, and are associated with worrisome selection of resistance upon repeated  
14 contact with treated surfaces (6).

15

16 Several studies have shown that non-antibiotic anti-adhesion strategies could  
17 also efficiently interfere with bacterial biofilm formation (7-14). The design of bio-  
18 inspired materials with anti-adhesion surface properties has been proposed to  
19 constitute an effective solution to protect patient care equipment, control  
20 pathogen colonization, and therefore impede key steps of infection, from initial  
21 surface contact to subsequent bacteria-bacteria interactions (15-17). Non-  
22 biocidal and bio-sourced strategies are also actively explored, including  
23 approaches preventing and/or disrupting biofilms based on the use of quorum  
24 sensing inhibitors that interfere with bacterial communications (18). Bacteria also  
25 secrete biosurfactants altering material surface properties such as wettability and  
26 charge (19, 20). These surface-active compounds reduce surface contacts and  
27 contribute to bacterial motility or are involved in competitive interactions between  
28 bacteria (12). Whereas many of these molecules correspond to small lipopeptides,  
29 recent studies showed that high molecular weight capsular polysaccharides  
30 released by various bacteria could prevent adhesion and subsequent cell  
31 aggregation and formation of biofilm by a wide range of Gram+ and Gram-  
32 bacteria. These include several nosocomial pathogens such as *Escherichia coli*,

1 *Pseudomonas aeruginosa*, *Klebsiella pneumoniae*, *Staphylococcus aureus*,  
2 *Staphylococcus epidermidis* and *Enterococcus faecalis* (7, 9, 11, 21-24).

3

4 Unlike secreted bacterial antagonistic macromolecules such as colicins, toxins,  
5 phages and a few toxic surface-active compounds (25, 26), these antibiofilm  
6 polysaccharides are non-biocidal (11). They impair bacteria-biotic/abiotic surface  
7 interactions mediated by adhesion factors such as pili, adhesins or extracellular  
8 matrix polymers via the modification of the wettability, charge and overall  
9 bacteria-surface contact properties (7, 12, 18). The use of these non-biocidal  
10 antibiofilm macromolecules was proposed as a promising resistance-free  
11 approach to reduce pathogenic biofilms and biofilm-associated bacterial  
12 infections while avoiding side effects caused by broad spectrum biocides (11, 23,  
13 27). However, the limited description of such antibiofilm macromolecules and  
14 their associated chemical and structural activities severely hinders their  
15 prophylactic use for bacterial biofilm control.

16

17 Here, we investigated the antibiofilm activity of a panel of 32 purified Gram+ or  
18 Gram- bacterial capsular polysaccharides of known composition and structure.  
19 Among those, we identified nine new non-biocidal polysaccharides inhibiting  
20 biofilm formation by prototypical nosocomial pathogens, including *E. coli* and *S.*  
21 *aureus*. This enabled us to perform a structure-function comparison of enough  
22 active and inactive polysaccharides and to show that antibiofilm capsular  
23 polysaccharides are characterized by a high intrinsic viscosity and a specific  
24 electrokinetic signature. Our study therefore identified key chemical and  
25 biophysical properties of bacterial antibiofilm polysaccharides, providing insights  
26 paving the way for engineering of new and well-defined non-biocidal surface-  
27 active macromolecules to control biofilm formation in medical and industrial  
28 settings.

29

30

31

## 1 **Results**

2

### 3 **Size integrity is a key parameter of antibiofilm polysaccharide activity**

4 To investigate the potential relationships between composition, structure, size  
5 and activity of non-biocidal bacterial antibiofilm polysaccharides, we first  
6 determined the structure of Group 2 capsule (G2cps), a previously identified  
7 hydrophilic and negatively charged antiadhesion polysaccharide active on both  
8 Gram+ and Gram- bacteria, which is naturally produced and released, notably,  
9 by uropathogenic *E. coli* strains (7). G2cps was purified by High-Performance  
10 Anion-Exchange Chromatography – Pulsed Amperometric Detection (HPAEC-  
11 PAD), High Performance Size-Exclusion Chromatography coupled to Static Light  
12 Scattering (HPSEC-LS) and analyzed by  $^1\text{H}$  and  $^{13}\text{C}$  nuclear two dimensional  $^1\text{H}$ -  
13  $^{31}\text{P}$  experiment magnetic resonance (NMR) studies. These analyses showed that  
14 G2cps polysaccharide consists of repeating units composed of O-acetylated and  
15 glycerol phosphate residues with an average molecular weight of 800 kDa as  
16 illustrated in Figure 1A. This structure is similar to that of *E. coli* polysaccharides  
17 K2 and K62 (also named K2ab) (28). We then gradually reduced the size of  
18 G2cps polysaccharide while preserving its structural integrity using radical  
19 oxidation hydrolysis (Supporting Figure S1). The determination of antibiofilm  
20 activity of full length and fragmented G2cps showed that even minor reduction of  
21 polysaccharide size resulted in a loss of G2cps activity (Figure 1B), indicating  
22 that the conservation of the size of the G2cps polymer is critical for its  
23 antiadhesion properties.

24

### 25 **Screening a collection of bacterial capsular polysaccharides reveals new** 26 **non-biocidal antibiofilm compounds**

27

28 To further attempt to identify G2cps structural or composition features associated  
29 with its activity, we screened a collection of 30 different high molecular-weight  
30 bacterial polysaccharides to detect new macromolecules with G2cps-like  
31 antibiofilm properties. Most of them are capsular polysaccharides of known origin,  
32 composition and structure produced and purified from different strains of  
33 *Streptococcus pneumoniae*, *Salmonella enterica* serovar Typhi, *Haemophilus*

1 *influenzae*, *Neisseria meningitidis*, and used as antigens in several  
2 polysaccharide and glycoconjugate human vaccines (Supporting Table S1). We  
3 showed that, at equal concentration (100µg/mL), Vi, MenA and MenC  
4 polysaccharides were as active as G2cps in inhibiting *E. coli* biofilm formation but  
5 were less active on *S. aureus* biofilms (Figure 2A, B). Moreover, whereas PRP  
6 and PnPS3 were active on both bacteria, the activity of PnPS12F was restricted  
7 to *E. coli* and that of PnPS18C to *S. aureus* (Figure 2A, B). The comparison of  
8 the activity of Vi, PRP, PnPS3, MenA and MenC showed that Vi is the most active  
9 polysaccharide and all 5 polysaccharides are non-biocidal (Supporting Figures  
10 S2 and S3). Finally, we confirmed the activity of Vi, MenA, PRP and PnPS3 on a  
11 panel of biofilm-forming Gram+ or Gram- bacteria, including a biofilm-forming *E.*  
12 *coli* K-12 MG1655 carrying a F conjugative plasmid, *Enterobacter cloacae* 1092,  
13 *K. pneumoniae* Kp21, *S. aureus* 15981 and *S. epidermidis* O47 (Supporting  
14 [Figure S4](#)).

15

### 16 **Polysaccharide conformation and high intrinsic viscosity are predictive** 17 **indicators of antibiofilm activity.**

18 To identify the structural and biophysical properties that potentially correlate with  
19 polysaccharide antibiofilm activity, we determined the molecular weight (*Mw*) and  
20 the intrinsic viscosity ( $[\eta]$ ) of active (Vi, MenA, MenC, PnPS3, PRP, G2cps) and  
21 inactive (PnPS1, PnPS8, PnPS19A, PnPS9V, PnPS7F, PnPS22F and PnPS14)  
22 polysaccharides by HPSEC (Table 1). Intrinsic viscosity  $[\eta]$  of a given  
23 polysaccharide reflects its contribution to the viscosity  $\eta$  of the whole solution, i.e.  
24  $[\eta]=(\eta-\eta_o)/(\eta_o \phi)$ , where  $\eta_o$  is the solution viscosity in the absence of  
25 polysaccharide and  $\phi$  stands for the volume fraction of polysaccharides in  
26 solution. Accordingly,  $[\eta]$  depends on the conformation adopted by the  
27 polysaccharides in solution. This conformation being itself mediated by several  
28 physicochemical parameters, including the electrostatic charges carried by the  
29 polysaccharide and the charge distribution within the macromolecular body. The  
30 combination of *Mw* and  $[\eta]$  parameters are indicative of the volume (per mass  
31 unit) occupied by the polysaccharides in solution. This analysis revealed a  
32 remarkable correlation between intrinsic viscosity and broad-spectrum antibiofilm

1 activity. Indeed, all inactive macromolecules systematically display the lowest,  
2 whereas active polysaccharides were characterized by a high ( $> 7$  dl/g) intrinsic  
3 viscosity (Supporting Figure S5). Moreover, molecular weight  $M_w$  and intrinsic  
4 viscosity  $[\eta]$  of polysaccharides with intermediate narrow-spectrum activity  
5 (PnPS18C and PnPS12F) cover range of values measured for both broad-  
6 spectrum active and non-active macromolecules. To determine whether high  
7 intrinsic viscosity could be indicative of a potential antibiofilm activity, we  
8 screened additional purified bacterial capsular polysaccharides of our collection  
9 and we identified two such non-biocidal polysaccharides, MenY and MenW135,  
10 presenting high intrinsic viscosity (Table 1 and Supporting Figures S3 and S5).  
11 Although MenY and MenW135 differ in their primary composition from Vi, MenA,  
12 MenC and G2cps, they both exhibited similar broad-spectrum antibiofilm activity  
13 (Figure 3 and Supporting Figure S6). These results indicated that specific  
14 polysaccharide conformation, reflected by a high intrinsic viscosity (29), is a  
15 determinant of antibiofilm activity.

16

### 17 **Active antibiofilm polysaccharides are highly negatively charged** 18 **macromolecules**

19 To further identify the molecular bases of the biophysical properties displayed by  
20 active polysaccharides, we first compared the composition of the broad-spectrum  
21 polysaccharides (Vi, MenA, MenW, MenY, MenC, G2cps, PRP, PnPS3) but could  
22 not identify a chemical feature common to all active molecules. Alternatively, we  
23 tested whether an increased surface hydrophilicity, previously associated with  
24 G2cps polysaccharide properties (7, 9), could correlate with the antibiofilm activity  
25 of the newly identified active polysaccharides. However, the determination of the  
26 surface contact angle of a drop of water on hydrophilic glass and hydrophobic  
27 plastic surfaces treated with either distilled deionized water or active and inactive  
28 polysaccharides did not reveal any correlation between surface  
29 hydrophilicity/hydrophobicity balance and antibiofilm activity (Supporting Figure  
30 S7). As an additional support of this finding, the characterization of  
31 polysaccharide-coated surfaces by Atomic Force Microscopy (AFM) operated in  
32 force spectroscopy mode using  $\text{CH}_3$ -functionalized nanometric tips did not reveal

1 any correlation between antibiofilm activity, structural surface patterns of  
2 adsorbed polysaccharides and surface hydrophobicity/hydrophilicity (Supporting  
3 Figure S8). We also evaluated the macromolecular charge, defined by a charge  
4 index  $i$  corresponding to the ratio between the number of acidic groups (carried  
5 by uronic and neuraminic acid groups or by phosphate groups) and the number  
6 of monosaccharide residues in a repeating unit (Table 1). The determination of  
7 this charge index showed that all active polysaccharides (Vi, MenA, MenW135,  
8 MenY, MenC, G2cps, PRP, PnPS3) correspond to highest  $i$ -values with  $i = 0.5$  or  
9 1. By contrast, macromolecules without anti-biofilm activity and with narrow-  
10 spectrum activity could not be differentiated based on their respective  $i$ -values.  
11 For instance, PnPS18C (narrow activity) for instance, shares similar value of  $i$  (=   
12 0.2) with PnPS9V and PnPS22F (no activity). These results suggested that the  
13 density of negative charges carried by the polysaccharides could be a key  
14 determinant of the biophysical properties associated with broad-spectrum  
15 antibiofilm activity.

16

### 17 **Active and inactive antibiofilm polysaccharides display distinct** 18 **electrokinetic patterns**

19 Previous reports documented the link between structure, surface charge  
20 organization and electrokinetic properties of macromolecules (30-32) as derived  
21 from electrophoresis. Bacterial polysaccharides are paradigms of ‘soft’  
22 macromolecules, i.e. polyelectrolytic assemblies defined by a 3-dimensional  
23 charge distribution, permeable to ions from the background electrolyte solution  
24 and to the electroosmotic flow developed under electrophoresis measuring  
25 conditions (30-32).

26 To determine whether the electrokinetic properties of polysaccharides (which  
27 includes both charge density and flow permeability features) are linked or not to  
28 their anti-biofilm activity, we performed blind measurements of the electrophoretic  
29 mobility ( $\mu$ ) as a function of NaNO<sub>3</sub> electrolyte concentration in solution (1mM to  
30 100mM range) for eight active, broad spectrum (Vi, MenA, MenW135, G2cps,  
31 PRP, PnPS3) or narrow spectrum (PnPS18C and PnPS12F) polysaccharides.  
32 The electrophoretic mobility of these active polysaccharides was then compared

1 to those of seven inactive polysaccharides (PnPS1, PnPS9V, PnPS8, PnPS19A,  
2 PnPS7F, PnPS22F and PnPS14) (Figure 4). All tested polysaccharides displayed  
3 the characteristic electrophoretic signature expected for soft macromolecules,  
4 with an electrophoretic mobility tending to a constant, non-zero mobility plateau  
5 value (noted below as  $\mu^*$ ) at sufficiently large salt concentrations (>30 mM). This  
6 property is the direct consequence of the penetration of the electroosmotic flow  
7 within the charged polysaccharide globular structure (33). Further qualitative  
8 inspection of the sets of electrokinetic data collected for the polysaccharides of  
9 interest revealed two main electrokinetic patterns. The first one corresponded to  
10 the 7 tested inactive macromolecules whose electrophoretic mobility  
11 systematically tends to value of  $\mu^*$  satisfying  $0.5 < |\mu^*| < 1.5 \times 10^{-8} \text{ m}^2 \text{ V}^{-1} \text{ s}^{-1}$ . For  
12 these macromolecules, the absolute value of the electrophoretic mobility  
13 decreases with increasing electrolyte concentration as a result of screening of the  
14 polysaccharide charges by the electrolyte ions. This feature is also shared by the  
15 active macromolecules (PnPS3, PRP and G2cps) with the noticeable difference  
16 that their asymptotic mobility value  $|\mu^*|$  is significantly larger with  $\mu^*$  now  
17 satisfying the inequality  $|\mu^*| > 2 \times 10^{-8} \text{ m}^2 \text{ V}^{-1} \text{ s}^{-1}$  (Figure 4A). The second observed  
18 electrokinetic pattern applies to macromolecules with narrow (PnPS18C and  
19 PnPS12F) or broad-spectrum (Vi, MenA, MenW135) activities and for which the  
20 electrophoretic mobility  $\mu$  poorly depends on background electrolyte  
21 concentration. Strikingly, active macromolecules with narrow spectrum antibiofilm  
22 activity are defined by electrophoretic mobilities ( $|\mu^*| < 0.5 \times 10^{-8} \text{ m}^2 \text{ V}^{-1} \text{ s}^{-1}$ ) that  
23 are much lower in magnitude compared to those measured for broad-spectrum  
24 antibiofilm polysaccharides (MenA, MenW135 and Vi,  $|\mu^*| > 2 \times 10^{-8} \text{ m}^2 \text{ V}^{-1} \text{ s}^{-1}$ )  
25 (Figure 4B). These results demonstrated clearly that active capsular  
26 polysaccharides are characterized by a specific electrokinetic signature.

27

### 28 **The electrokinetic signature of antibiofilm polysaccharides is associated to** 29 **their high flow permeability and high density of electrostatic charges**

30 To further explore the electrokinetic properties of active capsular polysaccharides  
31 we interpreted quantitatively the dependence of the electrophoretic mobility ( $\mu$ ) of  
32 the tested macromolecules on background electrolyte concentration with soft

1 surface electrokinetic theory. This theory was developed by Ohshima for the  
2 electrophoresis of soft colloids (33) in the Hermans-Fujita's limit that is applicable  
3 to soft polyelectrolytes (34) (eq 1 in Materials and Method section). To that end,  
4 the required hydrodynamic radii of the macromolecules of interest were  
5 determined by Dynamic Light Scattering (DLS) after conversion of the measured  
6 diffusion coefficients by means of Stokes-Einstein equation (See Methods and  
7 Supporting Table S2). This quantitative analysis highlighted an excellent  
8 reconstruction of the electrophoresis data measured for all tested  
9 macromolecules tested (Figure 4) and, most importantly, a remarkable  
10 classification of their activity (Figure 5) according to their electrostatic and flow  
11 permeability properties.

12 These properties are expressed by two key parameters retrieved from theoretical  
13 fitting of electrophoretic data to eq 1, namely:  $\rho_o$ , which is the net density of  
14 negative charges carried by the macromolecule, and  $\lambda_o$  the so-called softness  
15 parameter.  $1/\lambda_o$  (also called the Brinkman length) corresponds to the extent of  
16 penetration of the electroosmotic flow within the macromolecule.  $1/\lambda_o$  is intimately  
17 correlated to the polysaccharide structural compacity and by the degree of  
18 entanglement of its constituting chains. All macromolecules with narrow spectrum  
19 activity (PnPS18C and PnPS12F) are in the lower left zone within the diagram  
20 reporting the determined value of  $\rho_o$  as a function of the corresponding  $1/\lambda_o$   
21 (Figure 5). By contrast, polysaccharides with a broad-spectrum activity (e.g. Vi,  
22 MenA, MenW135, PRP, PnPS3, G2cps) combine high charge density and high  
23 Brinkman length scale, and they are thus found at the upper right region in the  
24  $\rho_o$ - $1/\lambda_o$  representation (Figure 5). All tested inactive macromolecules (PnPS1,  
25 PnPS9V, PnPS8, PnPS19A, PnPS7F, PnPS22F and PnPS14) are positioned in  
26 a region intermediate between those of the broad-spectrum active and narrow-  
27 spectrum active macromolecules. Taken together, our results indicate that  
28 despite the lack of specific molecular motif associated with antibiofilm properties,  
29 the combination of a loose structure (i.e. a large permeability to flow due to a  
30 large amount of intraparticulate voids) and a high density of carried electrostatic  
31 charges is critical for polysaccharides to exhibit antibiofilm activity.

## 1 DISCUSSION

2  
3 The inhibition of bacterial adhesion using surface-active compounds is  
4 considered a promising approach to prevent the key initial steps of bacterial  
5 biofilm formation. In this study, we identified nine new non-biocidal antibiofilm  
6 macromolecules among a collection of 30 different high molecular-weight  
7 bacterial capsular polysaccharides of known structure and composition. This  
8 allowed us to compare their chemical, structural and electrokinetic properties to  
9 identify key molecular and biophysical determinants discriminating active  
10 polysaccharides from inactive ones.

11 The identified active polysaccharides are composed of a high number of  
12 repeating oligosaccharides with different composition and structure. This  
13 suggests that, beyond the specific composition of the active polysaccharide, the  
14 determinant of their antibiofilm activity could lie in higher order molecular features.  
15 Consistently, we showed that, in the case of G2cps, the size integrity of the  
16 polysaccharide is critical to maintain antibiofilm activity. We also demonstrated  
17 that a high intrinsic viscosity is a property shared by broad spectrum active  
18 macromolecules, which displayed the highest charge index  $i$  among all tested  
19 polysaccharides tested. The hydrodynamic radii measured for all tested  
20 macromolecules was shown to cover a relatively narrow range, between ca. 15  
21 and 40 nm in hydrodynamic diameter (Supporting Table S2). Such small  
22 variations in particle size cannot account for the well differentiated range of  
23 intrinsic viscosity measured for non-active and active macromolecules (1 to 6 and  
24 7 to 12 dl/g, respectively, see Supporting Figure S5), especially since both active  
25 and non-active polysaccharides display identical molecular weight ranges  
26 (Supporting Figure S5). In contrast, the high intrinsic viscosities measured for  
27 active macromolecules correlate with their charge index  $i$ , indicative of a high  
28 charge density. This correlation could be due to the fact that viscosimetric  
29 properties of particle dispersions depend on their electrostatic characteristics that  
30 govern the extent of so-called primary and secondary electroviscous effects (35,  
31 36). These effects are a direct consequence of the presence of charged electric  
32 double layers (EDL) at the macromolecule/solution interface and of ensuing  
33 particle-particle and particle-fluid electrohydrodynamic interactions: the larger the

1 density of particle charges, the more significant electro-viscous effects become  
2 (38,39). As a consequence, the viscosity of a solution containing macromolecules  
3 of similar size can significantly differ according to the density of their carried  
4 electrostatic charges (35, 36). A large flow penetration within the particles body  
5 (as revealed by a high Brinkman length,  $1/\lambda_o$ , see Figure 5) is consistent with the  
6 existence of a relatively loose structure adopted by the macromolecules and a  
7 reduced frictional force they exert on electro-osmotic flow during electrophoresis,  
8 with a resulting significant electrophoretic mobility. Altogether, the identified  
9 properties of loose macromolecular structure combined with a high charge  
10 density and a related high intrinsic viscosity correlate with antibiofilm activity.

11

12 Analysis of the electrokinetic data revealed very distinct electrokinetic patterns  
13 associated with broad and narrow spectrum of antibiofilm activities, whereas  
14 inactive macromolecules exhibited an intermediate electrokinetic behavior  
15 (Figure 5). This suggests that the high and low magnitudes of the polysaccharide  
16 charges could determine their broad and narrow activity, respectively, since a  
17 charge density with magnitude lying in between these two extremes led to a loss  
18 of activity. However, we previously showed that, despite its high negative charge,  
19 G2cps displayed low affinity for cationic dyes (7), suggesting that its interaction  
20 with surrounding biotic or abiotic environment is not only driven by  
21 electrostatics ,but may also include remodeling of its surface properties. This  
22 could possibly include changes in surface hydration or steric repulsion, and  
23 subsequent limitation of bacterial adhesion (7). This indicates that consideration  
24 of polysaccharide electrostatic properties alone is not enough to account for their  
25 antibiofilm activity. Consistently, analysis of our electrokinetic data sets suggests  
26 indeed that the very organization of the polymer chains and the resulting flow  
27 permeability properties of the polysaccharidic macromolecules (as qualitatively  
28 indicated by the magnitude of their Brinkman length) play an important role in  
29 defining their antibiofilm activity. Considering that only charges located in the  
30 peripheral region of the macromolecules are probed by electrophoresis (35), the  
31 location of these charges and their degree of exposition to the outer solution are  
32 likely important factors underlying antibiofilm activity.

1 Then, how does polysaccharide molecular composition correlate with antibiofilm  
2 activity? Most active macromolecules display a high density of negative charges  
3 that could contribute to the electrostatic repulsion of negatively charged bacteria.  
4 However, bacterial surface structures such as pili, fimbriae, lipopolysaccharides  
5 or even poly-cationic exopolysaccharides are known to overcome these repulsive  
6 forces and promote bacterial adhesion and aggregation (37-39). We therefore  
7 hypothesize that the directionality of the interactions on surfaces (40) could be a  
8 critical determinant of broad spectrum antibiofilm polysaccharide activity. The  
9 proper exposition of electrostatic charges could optimize the steric repulsion  
10 effect in the antibiofilm macromolecules identified in this study. In addition, their  
11 high intrinsic viscosity and relative loose structure could mechanically modify the  
12 local conditions of adhesion and alter the perception of the surface by bacteria,  
13 thereby minimizing their adhesion in the presence of the identified  
14 polysaccharides (41). We therefore propose that the active antibiofilm  
15 polysaccharides identified in our study could have multi-pronged activity, with  
16 both short and long-range modifications of the surface-bacteria or bacteria-  
17 bacteria interactions, in particular via an alteration of the local adhesion  
18 conditions prevailing on the adhesion surface. The distinction between broad,  
19 narrow or lack of activity would therefore depend on the specific combination of  
20 biophysico-chemical properties displayed by each macromolecule.

21  
22 By providing a better definition of the chemical and structural basis of the broad-  
23 spectrum antibiofilm activity displayed by capsular polysaccharides, our study  
24 offers the possibility to identify new surface-active polysaccharides on the basis  
25 of their biophysical properties but also to design and engineer macromolecules  
26 mimicking antibiofilm polysaccharide activity through total or partial synthesis.  
27 These molecules could be used as non-biocidal biofilm control strategies in  
28 prophylactic treatment against the initial adhesion of biofilm-forming pathogens  
29 developing on medical and industrial materials.

30

## 1 MATERIALS AND METHODS

2

3 **Bacterial strains and growth conditions.** Bacterial strains used in this study  
4 are listed in Supporting Table S3. Gram- bacteria were grown in 0.4% glucose-  
5 M63B1 minimal medium (M63B1) or in lysogeny broth (LB) medium at 37°C, with  
6 appropriate antibiotics when required. Gram+ strains were cultured in tryptic soy  
7 broth (TSB) supplemented with 0.25% or 0.5% glucose (*E. cloacae*). Potential  
8 biocidal effect of antibiofilm polysaccharides was evaluated from growth curve  
9 determination in the presence of 100 µg/ml of purified polysaccharide.

10

11 **Bacterial polysaccharides.** *S. pneumoniae*, *N. meningitidis*, *S. Typhi* and *H.*  
12 *influenzae* capsular polysaccharides used in this study were obtained from Sanofi,  
13 Marcy l'Etoile France and Swiftwater, USA. *E. coli* polysaccharides were  
14 produced at the Institut Pasteur, Paris. Teichoic acid polysaccharide (cell wall PS,  
15 CWPS) from *Streptococcus pneumoniae* strain CSR SCS2 was from Statens  
16 Serum Institut (Ref 3459).

17

18 **Biofilm inhibition tests.** Overnight cultures were adjusted to an OD<sub>600nm</sub> of 0.05  
19 before inoculating 50 µl into 96-well polyvinyl chloride (PVC) plates (Falcon;  
20 Becton Dickinson Labware, Oxnard, CA) and added at a 1:1 ratio to 50 µl of filter-  
21 sterilized and purified polysaccharide at the desired concentration: i) 100 µg/ml  
22 for standardized antibiofilm activity experiments; ii) 3.125-100 µg/ml for test level  
23 of activity of the macromolecules. Biofilms were left to grow for 16 h at 37°C  
24 before quantification as described in (7).

25

26 **Polysaccharide purification.** G2cps polysaccharide was obtained from 24h  
27 cultures as described in (7). Briefly, CFT073 *E. coli* strains were grown in M63B1  
28 0.4%glucose for 24h at 37°C. After cold centrifugation at 7500 rpm for 10 minutes,  
29 supernatants were filtered through a 0.22µm filter. Polysaccharides were  
30 precipitated from cell-free supernatant using ice-cold ethanol (3:1 ratio ethanol /  
31 supernatant) followed by centrifugation for 2h at 10000 rpm and 4°C. Precipitated  
32 polysaccharides were resuspended and dialyzed against deionized water (10

1 kDa cassettes; Pierce, Rockford, IL). Total polysaccharide concentrations were  
2 measured by Duvois colorimetric assay (42). The polysaccharides were finally  
3 separated from residual lipopolysaccharides by gel filtration on Sepharose 6BCL  
4 column (GE Healthcare Life Sciences) in 1% sodium deoxycholate (43) and  
5 dualized against deionized water. Polysaccharide concentration was determined  
6 using High-Performance Anion-Exchange Chromatography with Pulsed  
7 Amperometry Detection (HPAEC-PAD) (Thermo Fischer Scientific, Dionex,  
8 Sunnyval, CA) as previously described(44).

### 11 **Polysaccharide structure analysis by High Performance Anion Exchange** 12 **Chromatography with Pulsed Amperometric Detection (HPAEC-PAD)**

13 Polysaccharide G2cps was hydrolyzed with hydrofluoric acid (HF) (48% by mass)  
14 for 16h at room temperature. HF was removed by drying under a stream of  
15 nitrogen at 40°C. The sample was redissolved in water and then hydrolyzed with  
16 2M trifluoroacetic acid (TFA) for 2h at 121°C. TFA was removed by drying under  
17 a stream of nitrogen at 40°C. The sample was redissolved in water prior to  
18 analysis. For the sake of comparison, both HF-alone and TFA-alone hydrolysis  
19 were also performed on polysaccharide G2cps. Pulsed amperometric detection  
20 was used incorporating a quadruple- potential waveform. Data were collected and  
21 analyzed on computers equipped with Dionex Chromeleon software (Dionex).  
22 Commercial monosaccharides were used as standards.

### 24 **Nuclear Magnetic Resonance (NMR) spectroscopy**

25 Approximately 5 mg of polysaccharide was lyophilized once, dissolved in 700 µl  
26 of deuterated water and 550 µl were introduced in a 5mm tube. NMR spectra  
27 were collected on a Bruker Avance 500MHz spectrometer running Topspin 2.1  
28 software at an indicated probe temperature of 20°C. Spectra were measured for  
29 solutions in D<sub>2</sub>O with 0.01% DSS as an internal standard for proton (<sup>1</sup>H) NMR (δ  
30 0.00 ppm). Phosphoric acid (2%) was used as an external standard for  
31 phosphorus (<sup>31</sup>P) NMR (δ 0.00 ppm) and TSP as an external standard for carbone  
32 (<sup>13</sup>C) NMR (δ 0.00 ppm). The pulse programs used were those in the Bruker

1 library except for the correlation spectroscopy (COSY) and total correlation  
2 spectroscopy (TOCSY) diffusion experiments. The diffusion delay was 80 ms for  
3 these two-dimensional experiments and the mixing time for the TOCSY was 100  
4 ms.

5 The two dimensional  $^1\text{H}$ - $^{31}\text{P}$  experiment was acquired using a  $J_{\text{H-P}}$  coupling value  
6 of 7Hz. The  $^1\text{H}$ - $^{13}\text{C}$  heteronuclear single quantum coherence (HSQC) spectra  
7 were acquired using a  $^nJ_{\text{H-C}}$  coupling value of 145Hz and a long range  $^nJ_{\text{H-C}}$   
8 coupling value of 5Hz for heteronuclear multiple bond correlation (HMBC).

9

### 10 **High Performance Size Exclusion Chromatography methods with triple** 11 **detection: $M_w$ and $[\eta]$ determinations**

12 Polysaccharides were analyzed at a concentration between 600 to 1000  $\mu\text{g/ml}$  in  
13 water. Analyses were performed using a TDA301 Viscotek HPSEC system  
14 consisting of an automated sampler with a HPLC pump with an injection loop of  
15 100  $\mu\text{l}$ , an on-line degasser, a viscometer, a refractive index (RI), and a right-  
16 angle laser light scattering detector (RALLS). The HPSEC analyses of  
17 polysaccharide were performed using TSK G4000 PWXL (0.7 $\times$ 30 cm) and TSK  
18 G6000 PWXL analytical columns (0.7 $\times$ 30 cm) connected in series at a flow rate  
19 of 0.5 ml/min, at 30°C. Tris buffer 2.5mM, pH 7.5 or phosphate buffer 200mM pH  
20 6.9 was used as mobile phase. The columns were kept at a constant temperature  
21 of 30°C. Omnisec software (Malvern) was used for data collection and data  
22 processing. This triple detection consisting of online RI, RALLS and viscometric  
23 detector was used to determine the molecular weight ( $M_w$ ) and the intrinsic  
24 viscosity ( $[\eta]$ ) of polysaccharides.

25

### 26 **Size reduction of G2cps polysaccharide**

27 75  $\mu\text{g}$  of polysaccharide were hydrolyzed in solution with ascorbic acid, copper  
28 and iron sulfate for 2 h at 30°C. Hydrolysis kinetics was followed by HPSEC  
29 analysis for 15 min, 1 h and 24 h.

30

1 **Contact angle measurements.** Glass or polyester plastic microscopy coverslip  
2 slides were treated with 80  $\mu$ l of distilled deionized water or with 100  $\mu$ g/ml  
3 solution of purified active and inactive polysaccharides. Slides were dried under  
4 a laminar flow hood and 2.5  $\mu$ l drops of water were deposited using a Kruss DSA4  
5 Drop Shape Analyzer on the surface of coated and uncoated slides, and contact  
6 angle was then measured 3 times.

7

8 **Atomic Force Microscopy measurements.**

9 Microscopy glass slides were treated with 100  $\mu$ g/ml solution of purified active  
10 and inactive polysaccharides for 10 minutes and rinsed with ultrapure water. AFM  
11 measurements were performed in ultrapure water, using a Fastscan Dimension  
12 Icon with Nanoscope V controller (Bruker). Images were obtained in Peak Force  
13 tapping mode, using gold-coated silicon nitride tips (NPG, Bruker), with a  
14 maximum applied force of 500 pN, a scan rate of 1 Hz, a peak force amplitude of  
15 300 nm and a peak force frequency of 2 kHz. For quantifying coated-surface  
16 hydrophobicity by means of chemical force microscopy, hydrophobic tips were  
17 prepared by immersing gold-coated silicon nitride tips (NPG, Bruker) for 12h in 1  
18 mM solution of dodecanethiol (Sigma) in ethanol, rinsed with ethanol and dried  
19 with N<sub>2</sub>. Spatial mappings were obtained by recording 32  $\times$  32 approach-retract  
20 force-distance curves on 5  $\mu$ m  $\times$  5  $\mu$ m areas, with a maximum applied force of  
21 500 pN and an approach and retraction speed of 500 nm/s.

22

23 **Electrokinetic measurements.**

24 1 g/L stock suspensions of macromolecules were first prepared in ultrapure water  
25 from corresponding frozen powders and, after 48 h, suspensions were diluted at  
26 250 mg/L and adjusted to pH 5. For each macromolecule tested, batches were  
27 then prepared in order to obtain a series of suspensions with NaNO<sub>3</sub> background  
28 electrolyte concentration in the range 1 to 100 mM. Final macromolecule  
29 concentration and pH conditions were adopted to optimize the measured  
30 electrophoretic response after testing a range of particle concentrations from 50  
31 to 250 mg/L and four pH conditions (3, 5, 7 and 9). All dispersions, stock and

1 diluted suspensions were stored at 4°C and were re-acclimatized at room  
 2 temperature prior to measurements.  
 3 24 to 48h after batches preparation, diffusion coefficients and electrophoretic  
 4 mobilities of the bacterial polysaccharides were measured by Dynamic Light  
 5 Scattering (DLS, Supporting Table S2) and Phase Analysis Light Scattering  
 6 (Malvern Instruments). Each reported data point in Figure 4 corresponds to three  
 7 measurements performed on 3 different aliquots of a given batch macromolecule  
 8 dispersion.

9

### 10 **Quantitative assessment of polysaccharide electrophoretic mobility.**

11 Electrophoretic mobility of the various macromolecules of interest were measured  
 12 as a function of NaNO<sub>3</sub> electrolyte concentration (Figure 4) and were collated with  
 13 the analytical theory developed by Ohshima for electrophoresis of soft colloids  
 14 (33) in the Hermans-Fujita limit applicable to soft polyelectrolytes (34). According  
 15 to the latter,  $\mu$  is defined by the expression

$$\begin{aligned}
 \mu = & \frac{\rho_o}{\eta\lambda_o^2} \left\{ 1 + \frac{1}{3} \left( \frac{\lambda_o}{\kappa} \right)^2 \left[ 1 + e^{-2\kappa b} - \frac{1 - e^{-2\kappa b}}{\kappa b} \right] \right. \\
 & \left. + \frac{1}{3} \left( \frac{\lambda_o}{\kappa} \right)^2 \frac{1 + 1/\kappa b}{(\lambda_o/\kappa)^2 - 1} \left[ \left( \frac{\lambda_o}{\kappa} \right) \frac{1 + e^{-2\kappa b} - (1 - e^{-2\kappa b})/\kappa b}{(1 + e^{-2\lambda_o b})/(1 - e^{-2\lambda_o b}) - 1/\lambda_o b} \right] - (1 - e^{-2\kappa b}) \right\} \quad (1)
 \end{aligned}$$

17 , where  $\rho_o$  represents the density of negative charges carried by the  
 18 macromolecule,  $\kappa$  is the reciprocal Debye layer thickness defined by

$$\kappa = \left[ 2F^2 c_o / (\varepsilon RT) \right]^{1/2}$$

19 with  $R$  the gas constant,  $T$  the absolute temperature,  $F$  the

20 Faraday number and  $c_o$  the bulk concentration of a 1:1 electrolyte (NaNO<sub>3</sub> in this  
 21 work),  $\lambda_o$  is the so-called softness parameter with  $1/\lambda_o$  corresponding to the  
 22 characteristic penetration length of the electroosmotic flow within the  
 23 macromolecule. The quantity  $b$  in eq 1 is the radius of the polyelectrolyte  
 24 macromolecule. The set of  $(\rho_o, 1/\lambda_o)$  couples obtained for all polysaccharidic  
 25 macromolecules are reported in Supporting Table S2 and the required values of

1 *b* for data fitting to eq 1 were determined by Dynamic Light Scattering and are  
2 also given in Supporting Table S2.

3

#### 4 **Statistical analysis.**

5 Two-tailed unpaired *t*-test with Welch correction analyses were performed using  
6 Prism 9.0 for Mac OS X (GraphPad Software). Each experiment was performed  
7 at least three times. All data are expressed as mean ( $\pm$  standard deviation, SD)  
8 in figures. Differences were considered statistically significant for *P* values of  
9  $<0.05$ ; \*  $p<0.05$ ; \*\*  $p<0.01$ ; \*\*\*  $p<0.001$ . \*\*\*\*  $p<0.0001$ .

## 10 **ACKNOWLEDGEMENTS**

11

12 We thank Olaya Rendueles for helpful discussions and Nadia Izadi and Laurence  
13 Mulard for critical reading of the manuscript. We are grateful to Heike Claus,  
14 Ulrich Vogel and Muhamed-kheir Taha, for generously providing us with  
15 assistance with some of the strains used in this study. This work was supported  
16 by a collaborative research grant Institut Pasteur and Sanofi, by grants from the  
17 French Government's Investissement d'Avenir program, Laboratoire  
18 d'Excellence "Integrative Biology of Emerging Infectious Diseases" (grant n°ANR-  
19 10-LABX-62-IBEID) and by the Fondation pour la Recherche Médicale (grant  
20 DEQ20180339185). J. B-B was the recipient of a long-term post-doctoral  
21 fellowship from the Federation of European Biochemical Societies (FEBS) and  
22 by the European Union's Horizon 2020 research and innovation program under  
23 the Marie Skłodowska-Curie grant agreement No 842629. This work was partly  
24 carried out in the Pôle de compétences Physico-Chimie de l'Environnement,  
25 LIEC laboratory UMR 7360 CNRS - Université de Lorraine.

26

27

## 1 REFERENCES

- 2
- 3 1. L. Hall-Stoodley, J. W. Costerton, P. Stoodley, Bacterial biofilms: from the natural
- 4 environment to infectious diseases. *Nat Rev Microbiol* **2**, 95-108 (2004).
- 5 2. H. C. Flemming, S. Wuertz, Bacteria and archaea on Earth and their abundance in
- 6 biofilms. *Nat Rev Microbiol* **17**, 247-260 (2019).
- 7 3. P. S. Stewart, J. W. Costerton, Antibiotic resistance of bacteria in biofilms. *Lancet* **358**,
- 8 135-138 (2001).
- 9 4. D. Lebeaux, J. M. Ghigo, C. Beloin, Biofilm-related infections: bridging the gap
- 10 between clinical management and fundamental aspects of recalcitrance toward
- 11 antibiotics. *Microbiology and molecular biology reviews : MMBR* **78**, 510-543 (2014).
- 12 5. K. Lewis, A. M. Klibanov, Surpassing nature: rational design of sterile-surface
- 13 materials. *Trends Biotechnol* **23**, 343-348 (2005).
- 14 6. P. N. Danese, Antibiofilm approaches: prevention of catheter colonization. *Chem Biol*
- 15 **9**, 873-880 (2002).
- 16 7. J. Valle *et al.*, Broad-spectrum biofilm inhibition by a secreted bacterial polysaccharide.
- 17 *Proc Natl Acad Sci U S A* **103**, 12558-12563 (2006).
- 18 8. A. K. Mukherjee, K. Das, Microbial surfactants and their potential applications: an
- 19 overview. *Adv Exp Med Biol* **672**, 54-64 (2010).
- 20 9. O. Rendueles *et al.*, Screening of *Escherichia coli* species biodiversity reveals new
- 21 biofilm-associated antiadhesion polysaccharides. *MBio* **2**, e00043-00011 (2011).
- 22 10. D. Campoccia, L. Montanaro, C. R. Arciola, A review of the biomaterials technologies
- 23 for infection-resistant surfaces. *Biomaterials* **34**, 8533-8554 (2013).
- 24 11. O. Rendueles, J. B. Kaplan, J. M. Ghigo, Antibiofilm polysaccharides. *Environ*
- 25 *Microbiol* **15**, 334-346 (2013).
- 26 12. O. Rendueles, J. M. Ghigo, Mechanisms of Competition in Biofilm Communities.
- 27 *Microbiol Spectr* **3** (2015).
- 28 13. A. Asadi, S. Razavi, M. Talebi, M. Gholami, A review on anti-adhesion therapies of
- 29 bacterial diseases. *Infection* **47**, 13-23 (2019).
- 30 14. M. Sarshar *et al.*, FimH and Anti-Adhesive Therapeutics: A Disarming Strategy Against
- 31 Uropathogens. *Antibiotics (Basel)* **9** (2020).
- 32 15. B. Schachter, Slimy business--the biotechnology of biofilms. *Nat Biotechnol* **21**, 361-
- 33 365 (2003).
- 34 16. A. L. Hook *et al.*, Combinatorial discovery of polymers resistant to bacterial
- 35 attachment. *Nat Biotechnol* **30**, 868-875 (2012).
- 36 17. C. Howell, A. Grinthal, S. Sunny, M. Aizenberg, J. Aizenberg, Designing Liquid-
- 37 Infused Surfaces for Medical Applications: A Review. *Adv Mater* **30**, e1802724 (2018).
- 38 18. O. Rendueles, J. M. Ghigo, Multi-species biofilms: how to avoid unfriendly neighbors.
- 39 *FEMS Microbiol Rev* 10.1111/j.1574-6976.2012.00328.x (2012).
- 40 19. T. R. Neu, Significance of bacterial surface-active compounds in interaction of bacteria
- 41 with interfaces. *Microbiol Rev* **60**, 151-166 (1996).
- 42 20. I. M. Banat *et al.*, Microbial biosurfactants production, applications and future potential.
- 43 *Appl Microbiol Biotechnol* **87**, 427-444 (2010).
- 44 21. M. Chmit *et al.*, Antibacterial and antibiofilm activities of polysaccharides, essential oil,
- 45 and fatty oil extracted from *Laurus nobilis* growing in Lebanon. *Asian Pac J Trop Med*
- 46 **7s1**, S546-552 (2014).
- 47 22. A. Chauhan *et al.*, Preventing biofilm formation and associated occlusion by
- 48 biomimetic glycocalyxlike polymer in central venous catheters. *J Infect Dis* **210**, 1347-
- 49 1356 (2014).
- 50 23. G. A. Junter, P. Thébault, L. Lebrun, Polysaccharide-based antibiofilm surfaces. *Acta*
- 51 *Biomater* **30**, 13-25 (2016).

- 1 24. B. Costa *et al.*, Broad-Spectrum Anti-Adhesive Coating Based on an Extracellular  
2 Polymer from a Marine Cyanobacterium. *Mar Drugs* **17** (2019).
- 3 25. R. M. Donlan, Preventing biofilms of clinically relevant organisms using bacteriophage.  
4 *Trends Microbiol* **17**, 66-72 (2009).
- 5 26. K. Tait, I. W. Sutherland, Antagonistic interactions amongst bacteriocin-producing  
6 enteric bacteria in dual species biofilms. *J Appl Microbiol* **93**, 345-352 (2002).
- 7 27. L. Travier, O. Rendueles, L. Ferrières, J. M. Herry, J. M. Ghigo, Escherichia coli  
8 resistance to nonbiocidal antibiofilm polysaccharides is rare and mediated by multiple  
9 mutations leading to surface physicochemical modifications. *Antimicrob Agents*  
10 *Chemother* **57**, 3960-3968 (2013).
- 11 28. K. Jann, B. Jann, M. A. Schmidt, W. F. Vann, Structure of the Escherichia coli K2  
12 capsular antigen, a teichoic acid-like polymer. *J Bacteriol* **143**, 1108-1115 (1980).
- 13 29. J. T. Yang, The viscosity of macromolecules in relation to molecular conformation. *Adv*  
14 *Protein Chem* **16**, 323-400 (1961).
- 15 30. A. Clements *et al.*, The major surface-associated saccharides of Klebsiella pneumoniae  
16 contribute to host cell association. *PLoS One* **3**, e3817 (2008).
- 17 31. J. F. Duval, V. I. Slaveykova, M. Hosse, J. Buffle, K. J. Wilkinson,  
18 Electrohydrodynamic properties of succinoglycan as probed by fluorescence correlation  
19 spectroscopy, potentiometric titration and capillary electrophoresis. *Biomacromolecules*  
20 **7**, 2818-2826 (2006).
- 21 32. J. F. L. Duval, F. Gaboriaud, Progress in electrohydrodynamics of soft microbial  
22 particle interphases. *Current Opinion in Colloid & Interface Science* **15**, 184-195  
23 (2010).
- 24 33. H. Ohshima, Electrophoresis of soft particles. *Advances in Colloid and Interface*  
25 *Science* doi.org/10.1016/0001-8686(95)00279-Y, 189-235 (1995).
- 26 34. J. J. Hermans, H. Fujita, *Koninkl. Ned. Akad. Wetenschap. Proc.* **B** 182 (1955).
- 27 35. F. S. Chan, J. Blachford, D. A. I. Goring, The secondary electroviscous effect in a  
28 charged spherical colloid. **22**, 378-385 (1966).
- 29 36. L. Zurita, F. Carrique, A. V. Delgado, The primary electroviscous effect in silica  
30 suspensions. Ionic strength and pH effects. *Colloids Surf., A* **92**, 23-28 (1994).
- 31 37. C. Berne, A. Ducret, G. G. Hardy, Y. V. Brun, Adhesins Involved in Attachment to  
32 Abiotic Surfaces by Gram-Negative Bacteria. *Microbiol Spectr* **3** (2015).
- 33 38. M. A. Daeschel, J. McGuire, Interrelationships between protein surface adsorption and  
34 bacterial adhesion. *Biotechnol Genet Eng Rev* **15**, 413-438 (1998).
- 35 39. S. L. Walker, J. A. Redman, M. Elimelech, Role of Cell Surface Lipopolysaccharides in  
36 Escherichia coli K12 adhesion and transport. *Langmuir* **20**, 7736-7746 (2004).
- 37 40. A. Beaussart *et al.*, Supported lysozyme for improved antimicrobial surface protection.  
38 *J Colloid Interface Sci* **582**, 764-772 (2021).
- 39 41. V. D. Gordon, L. Wang, Bacterial mechanosensing: the force will be with you, always.  
40 *J Cell Sci* **132** (2019).
- 41 42. M. Dubois, K. Gilles, J. K. Hamilton, P. A. Rebers, F. Smith, A colorimetric method for  
42 the determination of sugars. *Nature* **168**, 167 (1951).
- 43 43. X. X. Gu, C. M. Tsai, Purification of rough-type lipopolysaccharides of Neisseria  
44 meningitidis from cells and outer membrane vesicles in spent media. *Anal Biochem* **196**,  
45 311-318 (1991).
- 46 44. P. Talaga, M. Moreau, Quantification of C-polysaccharide in Streptococcus  
47 pneumoniae polysaccharides by high-performance anion-exchange chromatography  
48 with pulsed amperometric detection. *Dev Biol (Basel)* **103**, 27-34 (2000).
- 49

## TABLES

**Table 1: Relevant origin, and physicochemical properties of the polysaccharides used in this work.** Indicated values correspond to mean values.

Bacterial origin	Name	Mw' (kDa)	Intrinsic viscosity <sup>1</sup> [ $\eta$ ] (dl/g)	Charge index <i>i</i> *
<i>Escherichia coli</i> CFT073	G2cps	780	5-10	0.5
<i>Salmonella</i> Typhi	Vi	280	10	1
<i>Haemophilus influenzae</i> serotype b	PRP	550	10	0.5
<i>Neisseria meningitidis</i> serogroup A	MenA	200	10	1
<i>Neisseria meningitidis</i> serogroup C	MenC	200	10	1
<i>Neisseria meningitidis</i> serogroup Y	MenY	600	10	0.5
<i>Neisseria meningitidis</i> serogroup W135	MenW135	500	12	0.5
<i>Streptococcus pneumoniae</i> serotype 12F	PnPS12F	1000	10	0.16
<i>Streptococcus pneumoniae</i> serotype 18C	PnPS18C	300	3	0.2
<i>Streptococcus pneumoniae</i> serotype 1	PnPS1	850	4	0.33
<i>Streptococcus pneumoniae</i> serotype 3	PnPS3	700	7	0.5
<i>Streptococcus pneumoniae</i> serotype 9V	PnPS9V,	500	2	0.2
<i>Streptococcus pneumoniae</i> serotype 8	PnPS8	300	6	0.25
<i>Streptococcus pneumoniae</i> serotype 19A	PnPS19A	250	1	0.33
<i>Streptococcus pneumoniae</i> serotype 7F	PnPS7F	1000	1	0
<i>Streptococcus pneumoniae</i> serotype 22F	PnPS22F	800	2	0.2
<i>Streptococcus pneumoniae</i> serotype 14	PnPS14	500	1	0

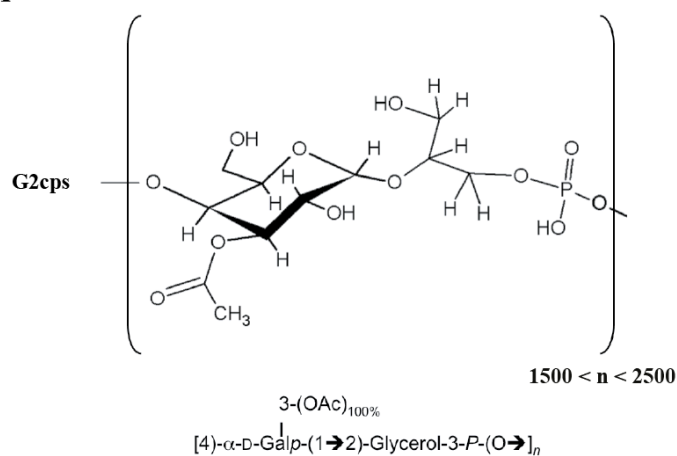
<sup>1</sup>: The relative standard deviation of Mw and [ $\eta$ ] determination is < 10%.

In red: active broad spectrum antibiofilm polysaccharides. In blue: active narrow spectrum antibiofilm polysaccharides. \* The charge index *i* corresponds to the ratio of the number of acidic group to the number of monosaccharide residue in a repeating unit.

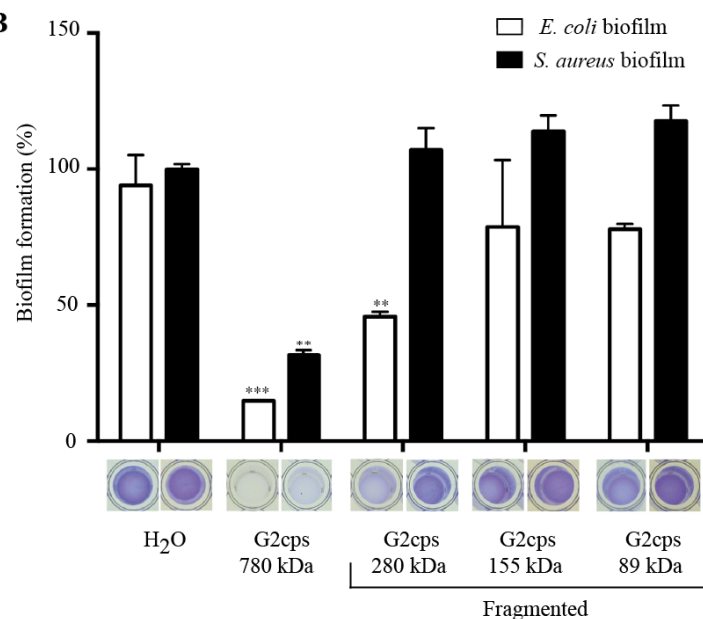
1 **FIGURES**

2

A



B



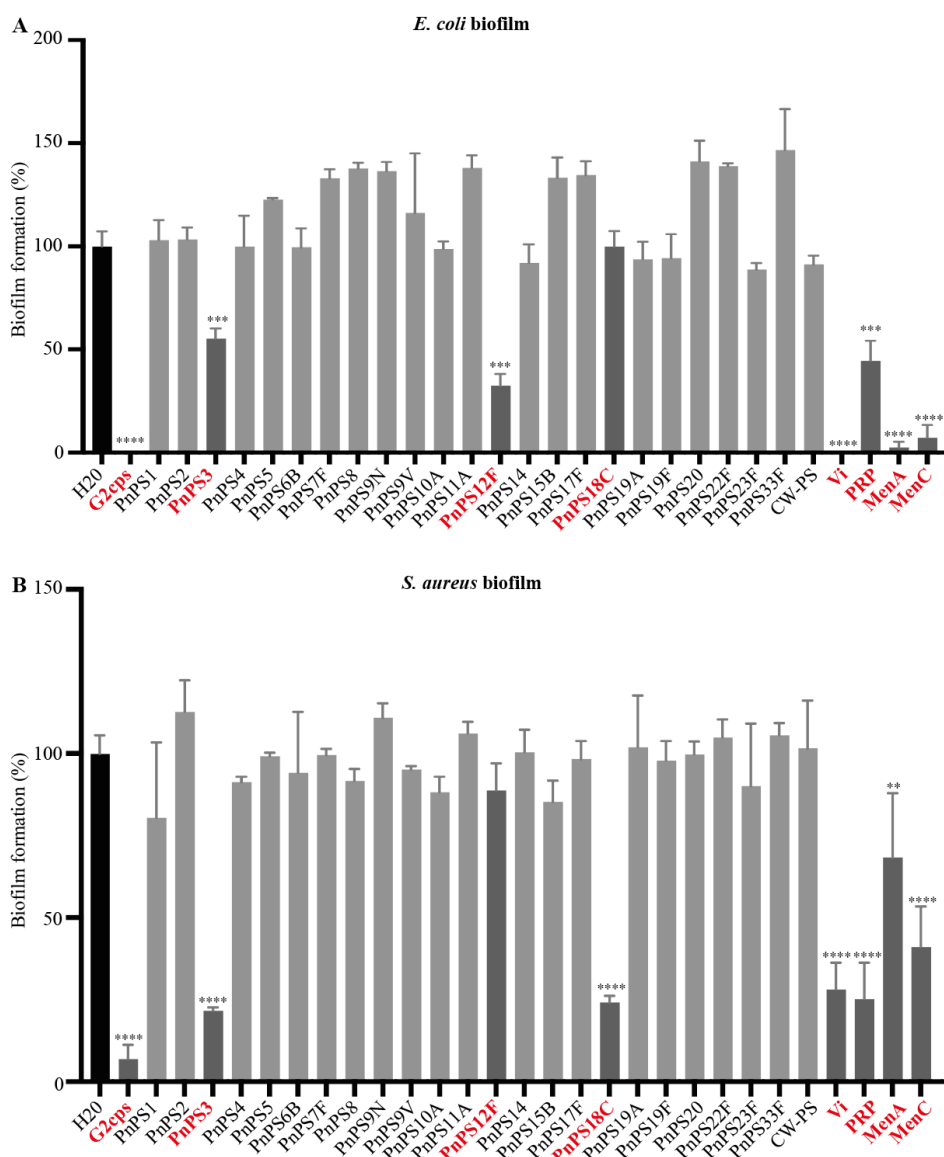
3

4

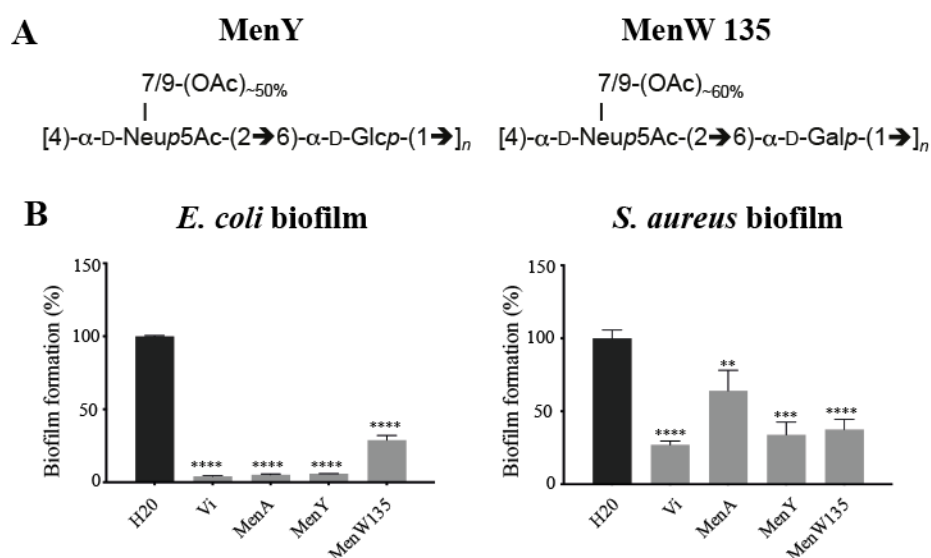
5 **Figure 1. Structure of the G2cps polysaccharide and its antibiofilm activity**  
 6 **as a function of the extent of its fragmentation. A.** Structure and composition  
 7 of G2cps polysaccharide. **B.** Biofilm inhibition activity against *E. coli* and *S.*  
 8 *aureus* biofilm of native and fragmented G2cps polysaccharide. Biofilm assays  
 9 were performed in the presence of 50 µg/ml of polysaccharide. Each experiment  
 10 was performed at least 3 times. \*\* p<0.01; \*\*\* p<0.001.

11

12

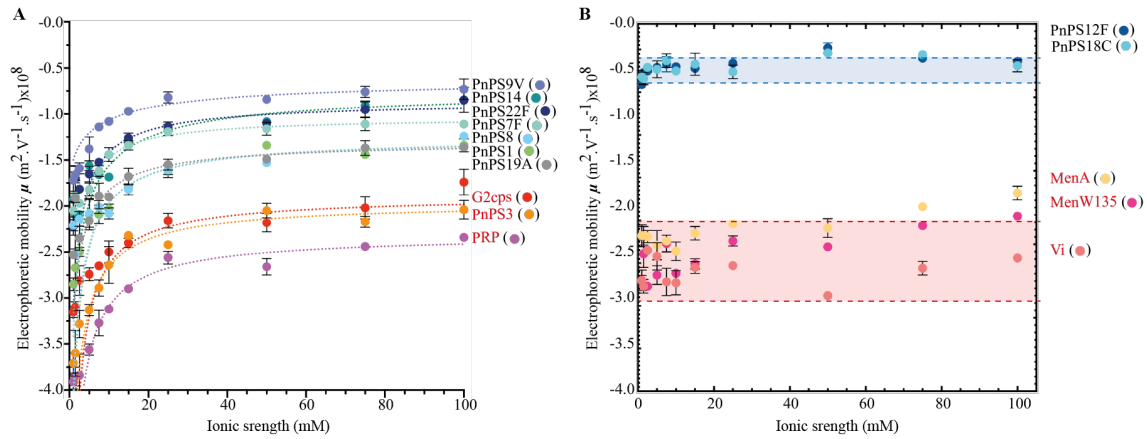


1  
2  
3 **Figure 2. Antibiofilm activity of a collection of bacterial polysaccharides.** *E.*  
4 *coli* (panel A) or *S. aureus* (panel B) biofilm formation assay in the presence of  
5 purified bacterial polysaccharides. G2cps was included as a positive control of  
6 active macromolecules and water was used as negative control. Red : active  
7 polysaccharides with Vi, MenA, MenC, G2cps , PRP and PnPS3 displaying broad  
8 spectrum of action, while PnPS18C is only active against Gram+ bacteria and  
9 PnPS12F against Gram- bacteria. Experiments were performed twice and in  
10 triplicate in presence of 100 µg/mL of each macromolecule. \*\* p<0.01; \*\*\*  
11 p<0.001; \*\*\*\* p<0.0001.  
12  
13



1  
2  
3  
4  
5  
6  
7  
8  
9  
10

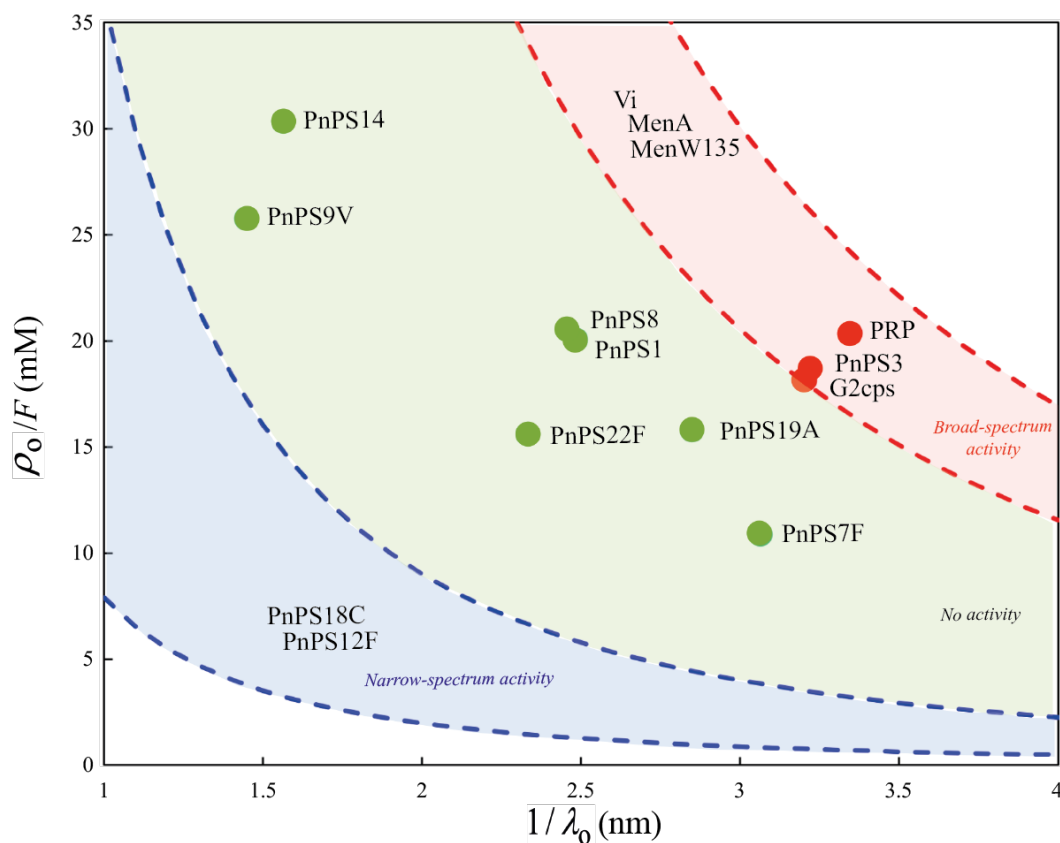
**Figure 3. MenA and MenY antibiofilm activity.** **A.** Chemical composition and acidic/hydrophobic group ratio of the *N. meningitidis* polysaccharides MenY and MenW135. **B.** Antibiofilm activity of MenY and MenW135 in comparison with previously identified active macromolecules. Biofilm inhibition tests were performed in presence of 50 µg/mL of polysaccharide. Distilled water was used as a negative control. Each experiment was performed at least 3 times. \*\* p<0.01; \*\*\* p<0.001; \*\*\*\* p<0.0001.



1  
2

3 **Figure 4. Dependence of the electrophoretic mobility of polysaccharides on**  
4 **NaNO<sub>3</sub> electrolyte concentration.** Points: experimental data. Dashed lines:  
5 theory (eq 1). **A:** Polysaccharides whose electrophoretic mobility significantly  
6 depends on solution ionic strength (fixed by NaNO<sub>3</sub> electrolyte concentration). **B:**  
7 Bacterial polysaccharides whose electrokinetic features poorly depend on  
8 electrolyte concentration. Polysaccharide with name in red display a broad-  
9 spectrum antibiofilm activity. PnPS12F and PnPS18C display a narrow spectrum  
10 antibiofilm activity (see Table S1). In panel B, the blue zone delimited by blue  
11 dotted lines bracket the quasi-electrolyte concentration-independent  
12 electrophoretic mobility values measured for the polysaccharides with narrow-  
13 spectrum activity. The red zone delimited by red dotted lines bracket the quasi-  
14 electrolyte concentration-independent electrophoretic mobility values measured  
15 for the polysaccharides with broad spectrum activity.

16  
17



1  
 2 **Figure 5. Classification of the antibiofilm activity of the tested**  
 3 **polysaccharides according to their charge density  $\rho_0$  and flow penetration**  
 4 **length scale  $1/\lambda_0$ .** The charge density  $\rho_0$  (in  $\text{C m}^{-3}$ ) is given here in the form of an  
 5 equivalent concentration of anionic charges defined by  $\rho_0/F$  (in mM) with  $F$  the  
 6 Faraday constant. The couple  $(\rho_0, 1/\lambda_0)$  associated to each macromolecule is  
 7 retrieved from the modelling of the dependence of measured electrophoretic  
 8 mobility on the electrolyte concentration in solution according to eq 1. The dotted  
 9 lines correspond to the set of solutions  $(\rho_0, 1/\lambda_0)$  to the equation  $\mu = \mu^*$  obtained for  
 10 the macromolecules PnPS18C and PnPS12F and for the macromolecules Vi,  
 11 MenW135 and MenA (see colored parts in Figure 4B) whose mobility  $\mu$  over the  
 12 whole range of electrolyte concentrations does not significantly deviate from the  
 13 mobility value  $\mu^*$  measured at large electrolyte concentrations (100 mM). For  
 14 these macromolecules, the poor dependence of  $\mu$  on electrolyte concentration  
 15 renders difficult any accurate evaluation of both  $\rho_0$ , and  $1/\lambda_0$  as electrokinetic data  
 16 fitting then reduces to solve one equation (eq 1) with two unknowns ( $\rho_0$  and  $1/\lambda_0$ ).  
 17 The space of solutions  $(\rho_0, 1/\lambda_0)$  associated with Vi, Men135, MenA and  
 18 PnPS18C, PnPS12F correspond to the red and blue zones, respectively. They  
 19 are delimited by dotted lines that correspond to the  $(\rho_0, 1/\lambda_0)$  solutions of the  
 20 equation  $\mu = \mu^*$  where  $\mu^*$  identifies with the polysaccharide mobilities marked by  
 21 the dotted lines represented in Figure 4B.  
 22